View metadata, citation and similar papers at core.ac.uk

brought to you by CORE

provided by Digital.CSIC

A multiple dating-method approach applied to the Sanabria Lake moraine complex (NW Iberian Peninsula, SW Europe)

Laura Rodríguez-Rodríguez[a], Montserrat Jiménez-Sánchez[a], María José Domínguez-Cuesta[a], Vincent Rinterknecht[b], Raimon Pallàs[c], Didier Bourlès[d], Blas Valero-Garcés[e]

[a]Dpto. Geología, Universidad de Oviedo, Arias de Velasco s/n, 33005 Oviedo, Spain

laurarr@geol.uniovi.es; +34 985102936 (corresponding author)

[b]Department of Earth and Environmental Sciences, University of St Andrews, Fife KY16 9AL, UK

[c]Dept. Geodinàmica i Geofísica, Universitat de Barcelona, 08028 Barcelona, Spain

[d] Aix Marseille Université, CNRS-IRD-Collège de France, UM34 CEREGE, 13545 Aix-en-Provence, France

[e] IPE-CSIC, Avda. Montañana 1005, 50059 Zaragoza, Spain

Abstract

New evidence in the NW region of the Iberian Peninsula (~42°N 6°W) of a glacial advance coeval with the global Last Glacial Maximum (LGM) of the Marine Isotope Stage 2 has been identified through a dataset of exposure ages based on 23 ^{10}Be concentration measurements carried out on boulder samples taken from a set of latero-frontal moraines. Results span the interval 19.2–15.4 ^{10}Be ka, matching the last deglaciation period when Iberia experienced the coldest and driest conditions of the last 25 ka, and are consistent with Lateglacial chronologies established in other mountain regions from SW Europe. The extent of the LGM stade identified in this work is similar to the local maximum ice extent stade recorded and dated as prior to 33 ka using radiocarbon and optically stimulated luminescence. This work showcases how multiple-dating approaches and detailed geomorphological mapping are required to reconstruct realistic palaeoglacier evolution models.

Key words

Cosmogenic dating, glacial geomorphology, ice cap, Last Glacial Maximum, Lateglacial, Sanabria, Iberian Peninsula.

1. Introduction

Evidence for asynchronism between the maximum advances of mountain glaciers and continental ice sheets is reported worldwide, suggesting that the dynamics of both ice systems responded differently to rapid changes in temperature and/or moisture supply (e.g. Gillespie and Molnar, 1995; Florineth and Schlüchter, 2000; Zreda et al., 2011). Ice sheets grew to their maximum position between 33 and 26.5 ka in response to climatic forcing from decreases in summer insolation, tropical Pacific sea surface temperatures and atmospheric CO_2 levels, and nearly all were at their Last Glacial Maximum (LGM) positions from 26.5 to 19-20 ka corresponding to minima in these forcings (Clark et al., 2009). The latter implies a longer time interval for the LGM episode than previous estimations based on the marine isotope and global sea level records (18 ^{14}C ka BP or 21 ka cal BP; Ehlers and Gibbard, 2007). Regional differences in maximum ice extent (Würmian MIE) and timing between mountain regions and the asynchrony with the global LGM hold significant information on cryosphere dynamics and palaeoclimatic evolution during the last glacial cycle. In the mountain regions of southern Europe, two chronological scenarios were proposed (Hughes and Woodward, 2008): (1) a local glacial maximum several thousands of years earlier than the LGM of Marine Isotope Stage 2 (MIS 2) based on evidence from northern Iberian Peninsula, Italian Apennines and Greece dated with radiocarbon, Uranium series, and optically stimulated luminescence (OSL) techniques, and (2) a local glacial maximum close or coeval with the global LGM based on evidence from central Iberian Peninsula, Pyrenees, Maritime Alps and Turkey dated through terrestrial cosmogenic nuclides (TCN). Such contrasting scenarios could be related to regional climate variability, but also to limitations or biases of the applied dating methods, as TCN methods consistently provided the youngest ages and radiocarbon and OSL the oldest ones (Hughes and Woodward, 2008).

In the Iberian Peninsula mountains (Figure 1), the current knowledge about the extent, timing and number of glacial stades during the last glacial cycle (ca. last 120 ka) has been recently reviewed (Calvet et al., 2011; Jiménez-Sánchez et al., 2013) and is summarized as follows: (1) in the Pyrenees the Würmian MIE occurred between 97 and 36 ka depending on the valleys considered (García-Ruiz et al., 2013; Lewis et al., 2009; Pallàs et al., 2010), in the Cantabrian Mountains it was prior to 38 ka (Jalut et al., 2010; Jiménez-Sánchez and Farias, 2002; Moreno et al., 2010; Serrano et al., 2012, 2013), and in the Sistema Central occurred between 33-26 ka (Carrasco et al., 2013; Palacios et al., 2010, 2012; Vieira, 2008); (2) a new glacial advance took place during the LGM recording a glacial advance similar in extent to previous local MIE in the eastern end of the southern Pyrenees (23-21 ka) (Delmas et al., 2008; Pallàs et al., 2006, 2010) and in the Sistema Central (22-19 ka) (Carrasco et al., 2013; Palacios et al., 2010, 2012) while shorter glacial advances were recorded in the northern Pyrenees (20-18 ka) (Delmas et al., 2011), the western end of the southern Pyrenees (García Ruiz et al., 2003; Lewis et al., 2009), and the Cantabrian Mountains (almost ice-free conditions in some valleys by 20 ka) (Jiménez-Sánchez and Farias, 2002); (3) frontal moraines coeval with the Oldest Dryas have been dated in the eastern Pyrenees and in the Sistema Central (Delmas et al., 2009; 2011; Pallàs et al., 2006, 2010; Palacios et al., 2010, 2012). In spite of all these new datasets, it remains unclear to what extent the differences in magnitude between local Würmian MIE and LGM stades might result from biases introduced by regional climate patterns, the dating methods, or even from uncertainties in the interpretation of the feature being dated. The later can be particularly significant for glacial sequences composed of till deposits arranged as sets of frontal moraines, since depending on their preservation they can be interpreted as resulting from: (i) a single glaciation or episode of glacial advance and retreat with deposition of recessional moraines close in age, or (ii) more than one glaciation with superimposed glacial records. In the last case the moraines forming the frontal moraine complex would be very different in age.

The Sanabria Lake moraine complex provides a unique glacier setting in the Iberian Peninsula to test these hypotheses. The occurrence of a well-preserved glacial sequence that includes a set of recessional moraines with related glaciolacustrine successions, allowed the combination of geomorphological techniques with several dating methods to establish the significance of the whole moraine complex. The aims of this paper are 1) to constrain the timing and extent of glaciers during the last glacial cycle by combining new moraine ^{10}Be surface exposure ages with the pre-existing ^{14}C and OSL datasets, 2) to discuss the relevance of the new local chronology, by comparing it with other palaeoclimate records of Iberia and SW Europe.

2. Regional Setting

The Sanabria Lake area in NW Iberian Peninsula is located in the east side of the Trevinca Massif, a mid-latitude mountain range which is free of ice at present (Figure 1). The massif highlands are characterized by a smooth topographic plateau reaching an altitude of 2128 m. The northern rim of the plateau is cut by north-facing glacial cirques, which connect with Alpine glacial valleys up to 7 km-long. To the south the plateau decreases in height and slope progressively to c. 1600 m, where two main troughs, the Bibei and Tera valleys are incised. These glacial valleys are 26 km and 23.5 km-long, and drain W and E respectively. Additionally, the plateau area is drained by minor glacial valleys arranged in a radial pattern (Figure 1).

An ice cap covered the plateau during the local MIE, lowering the equilibrium line altitude to 1687 m in the Tera outlet (Cowton et al., 2009). Moraine deposits can be divided into two groups according to their distribution: (i) moraine complexes below 1600 m marking the terminal zones of the glacial valleys, and (ii) cirque moraines at altitudes above 1700 m. We focus on an area of 45 km^2 in the terminal zone of the former Tera glacial outlet, where a moraine complex and ice-related deposits are particularly well-preserved around the Sanabria Lake (Figures 1 and 2). It includes: (i) a system of lateral moraines longer than 6 km that connects to the front with undifferentiated tills delineating the local MIE and (ii) remains of at least nine frontal moraines spreading over a distance of 2 km. Directly up-valley from this moraine complex, a 9 m-long sediment core retrieved from the deepest part of the Sanabria Lake shows a 1.8 m-thick basal unit with massive sands to banded silts and clays dated by ^{14}C AMS between 25.6 ± 0.4 and 14.5 ± 0.3 cal yr BP (Rodríguez-Rodríguez et al., 2011). Considering a proglacial origin for these facies, the frontal recessional moraine enclosing the lake must be older than the basal age of the lake and consequently, some of the moraines could represent different positions of the glacier front during the post-MIE glacial retreat prior to 25.6 ka. A > 12 m-long core from the San Martín ice-dammed deposit located out with the outermost left lateral moraine and interpreted as synchronous or subsequent to the local MIE, gives a minimum age of 21.8 ± 0.4 cal yr BP (Rodríguez-Rodríguez et al., 2011). Published radiocarbon ages obtained from other cores from small ponds in the eastern side of the Trevinca Massif also constrain minimum ages for local glacier retreat (Figure 2): (i) 15.7 ± 0.4 cal yr BP at Laguna de La Roya (Allen et al., 1996; Muñoz-Sobrino et al., 2013); (ii) 18.1 ± 0.4 cal yr BP at Laguna de las Sanguijuelas (Muñoz-Sobrino et al., 2004) and (iii) 14.2 ± 0.3 cal yr BP at Lleguna (Allen et al., 1996). Additional time constraints is provided by Pias site, in the western side of the Trevinca Massif, where a sedimentary sequence composed of fine-grained lacustrine deposits lying on poorly sorted sandy gravels interstratified with massive diamicton layers is well-preserved at the junction between the Bibei and Barxacoba glacial valleys. Three quartz samples retrieved from glacio-fluvial and glacio-lacustrine sand units less than 1-m thick were analyzed with OSL and yielded minimum ages of 27 ± 2 ka, 31 ± 3 ka, and 33 ± 3 ka for the regional MIE (Pérez-Alberti et al., 2011). Based on this information, we identify two groups of chronological data post-dating the local MIE in the Trevinca Massif: (i) previous to the LGM (OSL dates) and (ii) synchronous or younger than the LGM (radiocarbon dates, Table 1).

3. Methodology

A geomorphological map (at a 1:50.000 scale) was produced through photointerpretation and was used to reconstruct the MIE of local glaciers in the whole massif by using an ArcGIS database (v. 9.2) and the spreadsheet Profiler v.2 (Benn and Hulton, 2010). Ice profiles were numerically modeled along 31 profiles disposed radially from the ice cap margin to its source area along its outlet glaciers.

The TCN analysis was conducted in the Sanabria Lake moraine complex, where the outermost lateral moraines were presumably formed during the local Würmian MIE stade, while the inset ones recorded subsequent post-MIE ice front locations (Figures 1 and 2).

We selected 23 samples to investigate the minimum surface exposure age for the end of the Würmian MIE stade and for three other subsequent glacial fronts. The sampling selection was designed considering the relative chronology of the moraine complex to cover as complete as possible the history of the Pleistocene glaciations in the Tera Valley (eastern side of the Trevinca Massif). A total number of five moraines were sampled, two of them (TER and MAR) corresponding to the left lateral moraine which marks the local MIE (a total of eight boulders) and the others (SAN, TET and SAU) corresponding to three subsequent glacial fronts (five boulders each one). The shielding effect of till or snow cover, the underexposure of moraine boulders and the tilting of boulder surfaces was minimized by choosing only those boulders lying at the top of the crest and showing the largest size (volume greater than a cubic meter or > 1 m^3), a well anchored base (but protruding at least 1 m from the moraine surface), and a flat surface (table-type). The crystalline character of the bedrock in the Tera catchment, which is mainly composed of augen gneiss with quartz-rich streaks and granodiorites with quartz-rich veins up to 6 cm-thick, allowed getting samples very riched in quartz directly in the field. Shallow samples were taken manually with hammer and chisel. Angular elevation of the horizon was measured at each sampling site with a clinometer and the topographic shielding factors was calculated using the CRONUS-Earth calculator (version 1.1.) following Balco et al. (2008). The sample treatment was performed in the *Laboratori de Cosmonúclids Terrestres de la Universitat de Barcelona* (Spain). Samples were crushed and sieved to obtain the 0.25-1 mm grain fraction. Other mineral phases except quartz were removed from the samples by magnetic separation (dark minerals), froth floatation (mainly feldspars), and repeated leaching (Kohl and Nishiizumi, 1992). Aluminum content was analyzed through ICP-OES on sample aliquots at the *Centre Científic i Tecnològic de la Universitat de Barcelona* (CCiTUB). The aluminum content in all samples is < 250 ppm to ensure an efficient separation of Be and Al during column chromatography. Muscovite grains were removed through sample shaking with clean paper sheets and 3 extra acid-batches in order to reduce the Al-content in samples SAU01, MAR03 and SAN05. For each sample between 14-23 g of clean quartz grains were spiked with 200 mg of ^{9}Be carrier and completely digested in 48% HF. The carrier used was a commercial standard solution 1000 mg/l of beryllium oxide in hydrochloric acid 2% from the Scharlau Company (1.02g/cm^{3}). Beryllium fraction of each sample was extracted through column chromatography (Ditchburn and Whitehead, 1994).

All the ^{10}Be concentration measurements were performed at the ASTER AMS facility in Aix-en-Provence, France. The measured ^{10}Be/^{9}Be ratios were corrected for lab procedural blanks and calibrated with the NIST_27900 beryllium standard (Reference Material 4325, assigned value of $2.79 \pm 0.03 \times 10^{-11}$) and using a ^{10}Be half-life of $1.36 \pm 0.07 \times 10^{6}$ years (Nishiizumi et al., 2007). Analytical uncertainties are reported as 1σ and include uncertainties associated with AMS counting statistics, standard uncertainty (certification), and chemical blank measurements. ^{10}Be concentration in quartz samples (Tables 2 to 4) was calculated following Balco (2006), while the surface exposure ages were calculated with the Cronus online calculator v. 2.2.1 assuming no erosion (Balco et al., 2008; Balco, 2010). Maximum erosion rates were estimated by calculating the ratio between the height of protruding minerals from boulder surfaces and the corresponding exposure ages deduced for no erosion. Correcting exposure ages using the maximum erosion rate of 6.66×10^{-5} cm yr^{-1} yielded exposure ages older by only ~ 200 years. Boulder ages discussed in this work were not corrected for erosion nor snow/vegetation cover to ensure that the reported ages are treated as minimum exposure ages. Moraine ages were obtained as the error-weighted mean of the exposure ages calculated for its boulders in the constant production rate model. Only the oldest boulders of each moraine, whose exposure ages are overlapping at 1σ, were used to derive the error-weighted mean moraine ages (Figure 3): (i) TER-02, TER-05, MAR-03 for the TER-MAR moraine; (ii) SAN-02, SAN-04, SAN-05 for the SAN moraine; (iii) TET-01, TET-02, TET-03 for the TET moraine; and (iv) SAU-01, SAU-02 SAU- 04 for the SAU moraine. This TCN chronology is compared with pre-existing OSL and ^{14}C datasets in the discussion.

4. Results

The geomorphological map (Figure 1) summarizes the main glacial evidence on the Trevinca Massif and its relative chronology, allowing the reconstruction of the ice cap dimensions. Ice fronts reached altitudes between 1580 – 950 m, 1510 – 1110 m, 1290 – 980 m, and 1170 – 1060 m in the East, North, West and South sides of the massif, respectively. The lowest altitudes correspond to the Tera and Bibei valleys, where the glacial front fluctuations left remarkable sets of moraines. According to the ice surface model, glaciers extended 475 km^2 over the massif during the local MIE, reaching up to 200 m of ice thickness on the plateau and up to 450 m in the glacial valleys. The Sanabria Lake moraine complex indicates that the glacier outlet that flowed along the Tera valley was 23.5 km long during the local MIE and recorded a total length reduction of 3 km by the time of the SAU moraine deposition. The width of this glacier tongue, measured at the eastern part of the Sanabria Lake basin, changed from 3.7 km to 1.7 km between the local MIE and the SAU stade, while the ice thickness reduced ca. 130 m according to ice surface estimations made in the Tera Valley using the spreadsheet Profiler v.2 (Benn and Hulton, 2010).

A minimum age of 19.2 ± 1.8 ^{10}Be ka (n = 3) can be established for the gently sloped left lateral moraine (TER-MAR) (Figures 2 to 4; Tables 3 and 4). The SAN frontal moraine marks a subsequent glacial still stand or minor readvance no later than 17.7 ± 1.7 ^{10}Be ka (n = 3). The minimum age for the TET moraine, located in a small tributary of the main Tera Valley, suggests the lack of connection between glacier streams of both valleys by 17.2 ± 1.6 ^{10}Be ka ago (n = 3). Meanwhile, the overall retreating Tera ice front located downwards from the Sanabria over-deepened depression (today occupied by the Sanabria Lake) deposited another five frontal moraines. We report a minimum age of 15.7 ± 1.5 ^{10}Be ka (n = 3) for the SAU moraine, which dams modern day Sanabria Lake.

The lack of geomorphological features indicating the location of the ice margins at higher elevations than the TET moraine does not allow establishing a detailed paleogeographic model for each subsequent deglaciation stade.

5. Discussion

The minimum ^{10}Be ages cover the time interval 19.2 ± 1.8 to 15.7 ± 1.5 ^{10}Be ka (uncertainties include those associated with the analytical procedures and the production rate) and are consistent with the relative chronology derived from the geomorphological sequence (Figure 2). Combining the new ^{10}Be dataset with published ^{14}C AMS and OSL results from the whole massif, we have identified two glacial advances very close in extent. The oldest one is recorded by glacio-fluvial sediments at Pias site (western Trevinca Massif) which yielded OSL ages ~ 27-33 ka (Pérez-Alberti et al., 2011), suggesting the occurrence of a local MIE earlier than MIS 2. The youngest one is supported by our TCN results. According to the new set of minimum ^{10}Be ages, the whole moraine sequence was developed between 19.2–15.7 ka (Figure 2). The outermost TER-MAR lateral moraine yields a minimum age of 19.2 ± 1.8 ^{10}Be ka for the glacier retreat; the minimum age for the sedimentation onset in the San Martín valley (as a consequence of the moraine runoff blockage) was radiocarbon-dated as 21.8 ± 0.4 cal ka BP (Rodríguez-Rodríguez et al., 2011). Both minimum ages are consistent with a second glacial advance during the LGM of MIS 2 very close in extent to the previous MIE. The SAN moraine, located in a retreated position compared with the TER-MAR moraine, was dated at 17.7 ± 1.7 ^{10}Be ka, which is consistent with the minimum ^{14}C AMS age of 18.1 ± 0.4 cal ka BP obtained from Laguna de las Sanguijuelas located between both moraines (Muñoz-Sobrino et al., 2004) (Figure 2). The TET moraine was deposited shortly after, at a minimum age of 17.2 ± 1.6 ^{10}Be ka, marking the separation between the main Tera glacier and its eastern tributary. Between 17.7 and 15.7 ^{10}Be ka, the retreating ice front built up five frontal moraines. The SAU moraine damming the Sanabria Lake represents the youngest frontal moraine of this sequence and yields a minimum exposure age of 15.7 ± 1.5 ^{10}Be ka. The consistence between ages obtained from the boulders in each moraine and published radiocarbon data suggests that the ^{10}Be results are not significantly affected by moraine post-depositional erosion in this area.

The ^{14}C AMS age of 15.7 ± 0.4 cal yr BP obtained at the base of the lacustrine deposit known as Laguna La Roya, located at 1608 m altitude next to the eastern plateau edge, suggests that at least the southern part of the plateau could have been partly ice–free by the time of the SAU moraine deposition (Allen et al., 1996; Muñoz-Sobrino et al., 2013; Figure 2). This hypothesis is coherent with an ELA rising of about 100-150 m compared to the local MIE, which would have caused a drastic reduction (by more than 80 %) in the extent of the accumulation zone in the southern part of the plateau. Therefore, the ice flow inputs from the Segundera-Cárdena valley would have been reduced and the ice source area would have been located in the northern part of the Tera catchment where the plateau records its highest elevation (Figure 1). The basal ^{14}C AMS ages obtained at the Lleguna core (14.2 ± 0.3 cal yr BP; Allen et al., 1996) and at the top of the basal detrital unit of the Sanabria Lake core (14.5 ± 0.3 cal yr BP; Rodríguez-Rodríguez et al., 2011) would represent the timing of glacial front retreat from the eastern part of the Sanabria Lake.

We note that the new ^{10}Be ages and the published ^{14}C AMS dataset are generally consistent, but one question remains concerning the disparity between the minimum ages obtained for the base of the Sanabria Lake sequence (25.6 ka cal BP), the San Martín ice dammed deposit (21.8 ka cal BP) (Rodríguez-Rodríguez et al., 2011) and the TER-MAR lateral moraine (19.2 ^{10}Be ka) reported in this work. The Sanabria Lake sequence is considerably older than the TER-MAR moraine and its associated ice dammed deposit. A possible explanation is a local LGM stade (prior to 21.8 ka) advancing over the Sanabria Lake basin and eroding the upper part of the sedimentary sequence related to the previous Würmian MIE retreat (~33 ka). Although ice-push structures (folding, faults) were not found in the basal unit of the Sanabria core, the occurrence of iron oxide-rich intervals could suggest a sedimentary unconformity, otherwise difficult to identify in the massive sandy levels. Alternatively, basal ages of the Sanabria Lake and San Martin sequences (derived from bulk sediment samples) could be older than the enclosing sediments if any reworking had happened or if considerable reservoir effects had taken place. However, the consistence between the ^{14}C AMS data obtained from these sequences and the OSL ages obtained in the Pias site at the western side of the massif suggests that this is not likely to be the case.

There is a strong coherence between the Sanabria dataset and other mountain regions in the Iberian Peninsula. The Würmian MIE stade observed in the Sanabria area (prior to 33 ka) correlates with a similar stade documented in the Sistema Central ~ 200 km southwards (33-26 ka) (Carrasco et al., 2013; Domínguez-Villar et al., in press; Palacios et al., 2010, 2012; Vieira, 2008), but is younger than the one recorded in the Cantabrian Mountains ~ 100 km northwards (prior to 38 ka) (Jalut et al., 2010; Jiménez-Sánchez and Farias, 2002; Moreno et al., 2010; Serrano et al., 2012, 2013) and in the Pyrenees ~ 450 km northeastwards (97-36 ka) (García-Ruiz et al., 2013; Lewis et al., 2009; Pallàs et al., 2010; Peña et al., 2004). According to multi-proxy reconstructions based on Iberian lacustrine and marine records, cold and relatively wet conditions during the MIS 5 to MIS 4 transition were responsible for the MIE of glaciers, at least, in northern Iberia; a shift towards greater aridity during MIS 4 and MIS 3 would have been responsible for subsequent deglaciation (Moreno et al., 2012). The mountain glacial advance during the global LGM has also been recorded differently across Iberia, reaching quasi-MIE positions not only in Sanabria, but also in the eastern part of the southern Pyrenees (Pallàs et al., 2006, 2010; Delmas et al., 2008) or the Sistema Central (Carrasco et al., 2013; Palacios et al., 2010, 2012). In other areas, like the Cantabrian Mountains or the northern and southwestern Pyrenees, the glacial advance was clearly less extensive (e.g. Jiménez-Sánchez et al., 2013; Delmas et al., 2011). Subsequent glacial retreat in Sanabria started no later than 19.2 ^{10}Be ka and recorded several glacial front stabilizations until 15.7 ^{10}Be ka. This glacier evolution is consistent with palaeoclimate reconstructions based on speleothem and lacustrine sequences from the

Iberian Peninsula which indicate that the coldest and driest interval of the last 25 ka took place between 18.2 and 15.4 ka (Moreno et al., 2012) during the Lateglacial, coinciding with the Mystery Interval, a stadial that occurred during the earliest phase of the last deglaciation (17.5 to 14.5 cal ka BP) coevally with low boreal summer and high austral summer insolation and with low temperatures in Greenland (HE1) (Denton et al., 2005, 2006).

The Sanabria dataset is also coherent with glacial evidence from other mid-latitude mountains across SW Europe. In the Alps, the Late Würmian glaciation reached the Alpine lowlands between 30 ka and 21 ka and was followed by a series of glacial front stabilizations between 18 – 17 ka to 14.7 ka and 11.3 to 9.7 ka (Darnault et al., 2012; Ivy-Ochs et al., 2008 and references therein). In the Tatra Mountains (western Carpathians), three trimlines have been identified and constrained with cosmogenic isotope ^{36}Cl revealing that a post-LGM glacial retreat started no later than 21.5 ka and subsequent glacial advances occurred at ~ 17 and 12 ka (Makos et al., 2013). Minimum moraine ages based on U-Th analysis, carried out in secondary calcite cements, and thermo luminescence (TL) analysis obtained from glacio-fluvial sediments in the Pindus Mountains supported a LGM advance of glaciers considerably less extensive than other glacial advances associated to previous cold stages (MIS 6 and MIS 12) in northwestern Greece (Hughes et al., 2006; Woodward et al., 1995, 2008). Similar U-Th studies in the Montenegro Mountains (Dinaric Alps) also revealed a local LGM advance considerably less extensive than previous glaciations, followed by several glacial front stabilizations at 17, 13 and 12 ka (Hughes et al., 2010). Finally, cosmogenic isotope datasets based on ^{36}Cl from different mountain areas across Turkey support a LGM stade between 26 and 20.3 ka, followed by several glacial advances during the Lateglacial (Akçar et al., 2007; Sarikaya et al., 2009; Zahno et al., 2010).

In summary the available dates from the Sanabria Lake glacier record support: (i) at least two glacial advances close in extent (a double local MIE) during the last glacial cycle, the first one prior to 33 ka and the second one during the LGM of MIS 2; and (ii) a sequence of glacial front stabilizations between 19.2 and 15.4 ^{10}Be ka that is synchronous with the Lateglacial evolution of other mountain glaciers in southern Europe. Glacier evolution in southern latitudes is closely controlled by moisture availability and, at orbital time scales, to the latitudinal shifts of climate patterns. The North Atlantic Polar Front shift towards the South was more pronounced during MIS 2 than during MIS 4, pushing the prevailing westerly storms more to the south and reducing the precipitation in central and northern Europe accordingly (Florineth and Schlüter, 2000). The latter would explain a shorter extent of glacial advances in northern Iberian mountain areas, particularly the Cantabrian Mountains and the northwestern Pyrenees. Nevertheless, additional chronological data are needed to test this hypothesis, especially in the Cantabrian Mountains where available chronologies for the last glacial cycle are currently based on ^{14}C AMS and OSL.

6. Conclusions

New chronological data based on the cosmogenic nuclide ^{10}Be in the Sanabria area supports a sequence of moraines formed between 19.2 and 15.4 ^{10}Be ka, interpreted as the result of successive stabilizations during general retreat during the Lateglacial. This record constitutes additional evidence for a glacial episode coeval with the global LGM of MIS 2 in SW Europe. The combination of the geomorphological observations, published ^{14}C and OSL dates, and the new TCN results, suggests a double local MIE, since the local LGM advance might be close in extent compared to the previous Würmian MIE stade (33 ka).

Our chronology correlates well with: (i) published TCN chronologies established in other mountain areas of southern Europe; and (ii) palaeoclimatic reconstructions for Iberia, which indicate that the coldest and driest conditions for the last 25 ka took place during the Lateglacial, matching the Mystery Interval. This study demonstrates that the combination of geomorphological surveys and several dating techniques can help to constrain chronologies and develop more accurate palaeoglacial models, particularly in areas with complex moraine systems.

Acknowledgements

Research funded by Spanish CICYT projects LIMNOCAL–CGL2006-13327-C04-01, GRACCIE-CSD2007-0006, TOPOIBERIA-CSD2006-0041 (Consolider Ingenio Program), RISKNAT-2009SGR520, and *Fundación Patrimonio Natural CyL*. L. Rodríguez-Rodríguez is granted by the Severo Ochoa (FICYT–Asturias) and the FPU (Spanish MECD) programs. The AMS facility ASTER (CEREGE) is supported by the INSU/CNRS, the French MESR, and the CEA institute. We are grateful to M. Arnold, G. Aumaître, and K. Keddarouche for the AMS measurements and to the Administration of the Sanabria Natural Park for the sampling permissions.

References

Akçar, N., Yavuz, V., Ivy-Ochs, S., Kubik, P.W., Vardar, M., Shlüchter, C., 2007. Paleoglacial records from Kavron Valley, NE Turkey: Field and cosmogenic exposure dating evidence. Quaternary International 164–165, 170–183.

Allen, J.R.M., Huntley, B., Watts, W. A., 1996. The vegetation and climate of northwest Iberia over the last 14,000 yr. Journal of Quaternary Science 11, 125–147.

Balco, G., 2006. Converting Al and Be isotope ratio measurements to nuclide concentrations in quartz. Available at: https:// hess.ess.washington.edu (accessed April 2012)

Balco, G., 2010. ^{26}Al – ^{10}Be exposure age/erosion rate calculators: update of constants file from 2.2 to 2.2.1. Available at: https:// hess.ess.washington.edu (accessed April 2012)

Balco, G., Stone, J., Lifton, N.A., Dunai, T., 2008. A complete and easily accessible means of calculating surface exposure ages or erosion rates from ^{10}Be and ^{26}Al measurements. Quaternary Geochronology 3, 174-195.

Benn, D. I. Hulton, N. R. J., 2010. An Excel™ spreadsheet program for reconstructing the surface profile of former mountain glaciers and ice caps. Computers & Geosciences 36, 605-610.

Calvet, M., Delmas, M., Gunnell, Y., Braucher, R., Bourlès, D., 2011. Recent advances in research on Quaternary glaciations in the Pyrenees. Developments in Quaternary Science 15, 127-139.

Carrasco, R. M., Pedraza, J., Domínguez-Villar, D., Villa, J., Willenbring, J. K., 2013. The plateau glacier in the Sierra de Béjar (Iberian Central System) during its maximum extent. Reconstruction and chronology. Geomorphology 196, 83-93.

Clark, P. U., Dyke, A. S., Shakun, J. D., Carlson, A. E., Clark, J., Wohlfarth, B., Mitrovica, J. X., Hostetler, S. W., McCabe, A. M., 2009. The Last Glacial Maximum. Science 325, 710–714.

Cowton, T., Hughes, P. D., Gibbard, P. L., 2009. Palaeoglaciation of Parque Natural Lago de Sanabria, northwest Spain. Geomorphology 108, 282-291.

Darnault, R., Rolland, Y., Braucher, R., Bourlès, D., Revel, M., Sánchez, G., Bouissou, S., 2012. Timing of the last deglaciation revealed by receding glaciers at the Alpine-scale: impact on mountain geomorphology. Quaternary Science Reviews 31, 127-142.

Delmas, M., Gunnell, Y., Braucher, R., Calvet, M., Bourlès, D., 2008. Exposure ages chronology of the last glaciation in the eastern Pyrenees. Quaternary Research 69, 231-241.

Delmas, M., Calvet, M., Gunnell, Y., 2009. Variability of Quaternary glacial erosion rates – A global perspective with special reference to the Eastern Pyrenees. Quaternary Science Reviews 28, 484-498.

Delmas, M., Calvet, M., Gunnell, Y., Braucher, R., Bourlès, D., 2011. Palaeogeography and ^{10}Be exposure-age chronology of Middle and Late Pleistocene glacier systems in the northern Pyrenees: Implications for reconstructing regional palaeoclimates. Palaeogeography, Palaeoclimatology, Palaeoecology 305, 109-122.

Denton, G.H., Alley, R.B., Comer, G.C., Broecker,W.S., 2005. The role of seasonality in abrupt climate change. Quaternary Science Reviews 24, 1159-1182.

Denton, G.H., Broecker, W., Alley, R.B., 2006. The mystery interval 17.5 to 14.5 kyr ago. In Brigham-Grette, J., Kull, C., Kiefer, T. (Eds.), PAGES News, 14-16.

Ditchburn, R. G., Whitehead, N. E., 1994. The separation of ^{10}Be from silicates. 3d Workshop of the South Pacific Environmental Radioactivity Association, 4-7.

Domínguez-Villar, D., Carrasco, R.M., Pedraza, J., Cheng, H., Edwards, R.L., Willenbring, J.K., in press. Early maximum extent of paleoglaciers from Mediterranean mountains during the last glaciation. Scientific Reports 3, 2034; DOI:10.1038/srep02034(2013).

Ehlers, J., Gibbard, P. L., 2007. The extent and chronology of Cenozoic Global Glaciation. Quaternary International 164-165, 6-20.

Florineth, D., Schlüchter, C., 2000. Alpine evidence for Atmospheric Circulation Patterns in Europe during the Last Glacial Maximum. Quaternary Research 54, 295-308.

García-Ruiz, J. M., Valero-Garcés, B. L., Martí-Bono, C., González-Sampériz, P., 2003. Asynchroneity of maximum glacier advances in the central Spanish Pyrenees. Journal of Quaternary Science 18, 61-72.

García-Ruiz, J. M., Martí-Bono, C., Peña-Monné, J. L., Sancho, C., Rhodes, E. J., Valero-Garcés, B., González-Sampériz, P., Moreno, A., 2013. Glacial and fluvial deposits in the Aragón Valley, central-western Pyrenees: Chronology of the Pyrenean late Pleistocene glaciers. Geografiska Annaler 95A (1), 15-32.

Gillespie, A., Molnar, P., 1995. Asynchronous maximum advances of mountain and continental glaciers. Reviews of Geophysics 33 (3), 311-364.

Hughes, P. D., Woodward, J. C., 2008. Timing of glaciation in the Mediterranean mountains during the last cold stage. Journal of Quaternary Science 23 (6-7), 575-588.

Hughes, P D., Woodward, J C., Gibbard, P.L., Macklin, M., Gilmour, M., Smith. G., 2006. The Glacial History of the Pindus Mountains, Greece. Journal of Geology 114, 413-434.

Hughes, P. D., Woodward, J. C., van Calsteren, P. C., Thomas, L. E., Adamson, K. R., 2010. Pleistocene ice caps on the coastal mountains of the Adriatic Sea. Quaternary Science Reviews 29, 3690-3708.

Ivy-Ochs, S., Kerschner, H., Reuther, A., Preusser, F., Heine, K., Maisch, M., Kubik, P., Schlüchter, C., 2008. Chronology of the last glacial cycle in the European Alps. Journal of Quaternary Science 23, 559-573.

Jalut, G., Turu i Michels, V., Deboubat, J. J., Otto, T., Ezquerra, J., Fontugne, M., Belet, J. M., Bonnet, L., Garcia de Celis, G., Redondo-Vega, J. M., Vidal-Romaní, J. R., Santos, L., 2010. Paleoenvironmental studies in NW Iberia (Cantabrian range): vegetation history and synthetic approach of the last deglaciation phases in the western Mediterranean. Palaeogeography, Palaeoclimatology, Palaeoecology 297 (2), 330-350.

Jiménez-Sánchez, M., Farias, P., 2002. New radiometric and geomorphologic evidence of Last Glacial maximum older than 18 ka in SW European Mountains: the example of Redes Natural Park, Cantabrian Mountains, NW Spain. Geodinamica Acta 15, 93-101.

Jiménez-Sánchez, M., Rodríguez-Rodríguez, L., García-Ruiz, J. M., Domínguez-Cuesta, M. J., Farias, P., Valero-Garcés, B., Moreno, A., Rico, M., Valcárcel, M., 2013. A review of glacial geomorphology and chronology in northern Spain: timing and regional variability during the last glacial cycle. Geomorphology 196, 50-64.

Kohl, C. P., Nishiizumi, K., 1992. Chemical isolation of quartz for measurement of *in-situ*-produced cosmogenic nuclides. Geochimica et Cosmochimica Acta 56, 3583-3587.

Lewis, C. J., McDonald, E. V., Sancho, C., Peña, J. L., Rhodes, E. J., 2009. Climatic implications of correlated Upper Pleistocene glacial and fluvial deposits on the Cinca and Gállego Rivers (NE Spain) based on OSL dating and soil stratigraphy. Global and Planetary Change 67, 141-152.

Makos, M., Nitychoruk, J., Zreda, M., 2013. Deglaciation chronology and paleoclimate of the Pięciu Stawów Polskich/Roztoki Valley, high Tatra Mountains, Western Carpathians, since the Last Glacial Maximum, inferred from ^{36}Cl exposure dating and glacier-climate modeling. Quaternary International 293, 63-78.

Moreno, A., Valero-Gracés, B. L., Jiménez-Sánchez, M., Domínguez, M. J., Mata, P., Navas, A., González-Sampériz, P., Stoll, H., Farias, P., Morellón, M., Corella, P., Rico, M., 2010. The last deglaciation in the Picos de Europa National Park (Cantabrian Mountains, northern Spain). Journal of Quaternary Science 25 (7), 1076-1091.

Moreno, A., González-Sampériz, P., Morellón, M., Valero-Garcés, B., Fletcher, W. J., 2012. Northern Iberian abrupt climate change dynamics during the last glacial cycle: A view from lacustrine records. Quaternary Science Reviews 36, 139-153.

Muñoz-Sobrino, C., Ramil-Rego, P., Gómez-Orellana, L., 2004. Vegetation of the Lago de Sanabria area (NW Iberia) since the end of the Pleistocene: a palaecological reconstruction on the basis of two new pollen sequences. Vegetation History and Archaeobotany 13, 1-22.

Muñoz-Sobrino, C., Heiri, O., Hazekamp, M., van der Velden, D., Kirilova, E.P., García-Moreiras, I., Lotter, A.F., 2013. Quaternary Science Reviews 80, 58 - 77.

Nishiizumi, K., Imamura, M., Caffee, M. W., Southon, J. R., Finkel, R. C., McAninch, J., 2007. Absolute calibration of ^{10}Be AMS standards. Nuclear Instruments and Methods in Physics Research B 258, 403-413.

Palacios, D., Marcos, J., Vázquez-Selem, L., 2010. Last Glacial Maximum and deglaciation of Sierra de Gredos, central Iberian Peninsula. Quaternary International 233 (1), 16-26.

Palacios, D., Andrés, N., Marcos, J., Vázquez-Selem, L., 2012. Glacial landforms and their paleoclimatic significance in Sierra de Guadarrama, Central Iberian Peninsula. Geomorphology 139-140, 67-78.

Pallàs, R., Rodés, A., Braucher, R., Carcaillet, J., Ortuño, M., Bordonau, J., Bourlès, D., Vilaplana, J.M., Masana, E., Santanach, P., 2006. Late Pleistocene and Holocene glaciation in the Pyrenees: a critical review and new evidence from ^{10}Be exposure ages, south-central Pyrenees. Quaternary Science Reviews 25, 2937-2963.

Pallàs, R., Rodés, A., Braucher, R., Bourlès, D., Delmas, M., Calvet, M., Gunnell, Y., 2010. Small isolated glacial catchments as priority target for cosmogenic surface dating of Pleistocene climate fluctuations, SE Pyrenees. Geology 38, 891–894.

Pérez-Alberti, A., Valcárcel-Díaz, M., Martini, I. P., Pascucci, V., Andrucci, S., 2011. Upper Pleistocene glacial valley-junction sediments at Pias, Trevinca Mountains, NW Spain, In: Martini, I. P., French, H. M., Pérez-Alberti, A. (Eds.), Ice-Marginal and Periglacial Processes and Sediments, Geological Society, London, Special Publication 354, pp. 93-110.

Rodríguez-Rodríguez, L., Jiménez-Sánchez, M., Domínguez-Cuesta, M. J., Rico, M. T., Valero-Garcés, B., 2011. Last deglaciation in northwestern Spain: New chronological and geomorphologic evidence from the Sanabria region. Geomorphology 135, 48-65.

Sarikaya, M., Zreda, M., Çiner, A., 2009. Glaciations and paleoclimate of Mount Erciyes, central Turkey, since the Last Glacial Maximum, inferred from ^{36}Cl cosmogenic dating and glacier modeling. Quaternary Science Reviews 28, 2326-2341.

Serrano, E., González-Trueba, J. J., González-García, M., 2012. Mountain glaciation and paleoclimate reconstruction in the Picos de Europa (Iberian Peninsula, SW Europe). Quaternary Research 78, 303-314.

Serrano, E., González-Trueba, J. J., Pellitero, R., González-García, M., Gómez-Lende, M., 2013. Quaternary glacial evolution in the Central Cantabrian Mountains (Northern Spain). Geomorphology 196, 65-82.

Vieira, G., 2008. Combined numerical and geomorphological reconstruction of the Serra da Estrela plateau icefield, Portugal. Geomorphology 97, 190-207.

Weninger, B., Jöris, O., 2008. A ^{14}C age calibration curve for the last 60 ka: the Greenland-Hulu U/Th timescale and its impact on understanding the Middle to Upper Paleolithic transition in western Eurasia. Journal of Human Evolution 55, 772-781.

Weninger, B., Jöris, O., Danzeglocke, U., 2007. CalPal-2007. Cologne Radiocarbon Calibration and Palaeoclimate Research Package. Available at: http://222.calpal.de/2007 (May 2012)

Woodward, J. C., Lewin, J., Macklin, M.G., 1995. Glaciation, river behaviour and the Palaeolithic settlement of upland northwest Greece. In Lewin, J., Macklin, M.G., Woodward, J.C., (Eds.) Mediterranean Quaternary River Environments, Rotterdam, Balkema: 115-129.

Woodward, J. C., Hamlin, R.H.B., Macklin, M.G., Hughes, P.D., Lewin, J., 2008. Glacial activity and catchment dynamics in northwest Greece: Long-term river behaviour and the slackwater sediment record for the last glacial to interglacial transition. Geomorphology 101, 44-67.

Zahno, C., Akçar, N., Yavuz, V., Kubik, P. W., Schlüchter, C., 2010. Chronology of Late Pleistocene glacier variations at the Uludağ Mountain, NW Turkey. Quaternary Science Reviews 29, 1173-1187.

Zreda, M., Çiner, A., Akif Sarikaya, M., Zweck, C., Bayari, S., 2011. Remarkably extensive glaciation and fast deglaciation and climate change in Turkey near the Pleistocene-Holocene boundary. Geology 39, 1051-1054.

Figure 1. (a) Setting (1- Pyrenees, 2- Cantabrian Mts., 3- Sistema Central, 4- Trevinca Massif). (b) Geomorphological map of the Trevinca Massif, including published ages: radiocarbon data (1-5) (see also Table 1) and optically stimulated luminescence data (OSL) from Pias site (6-8; Pérez-Alberti et al., 2011). The rectangle indicates Figure 2 location. (c) Ice cap reconstruction for the local maximum ice extent (MIE).

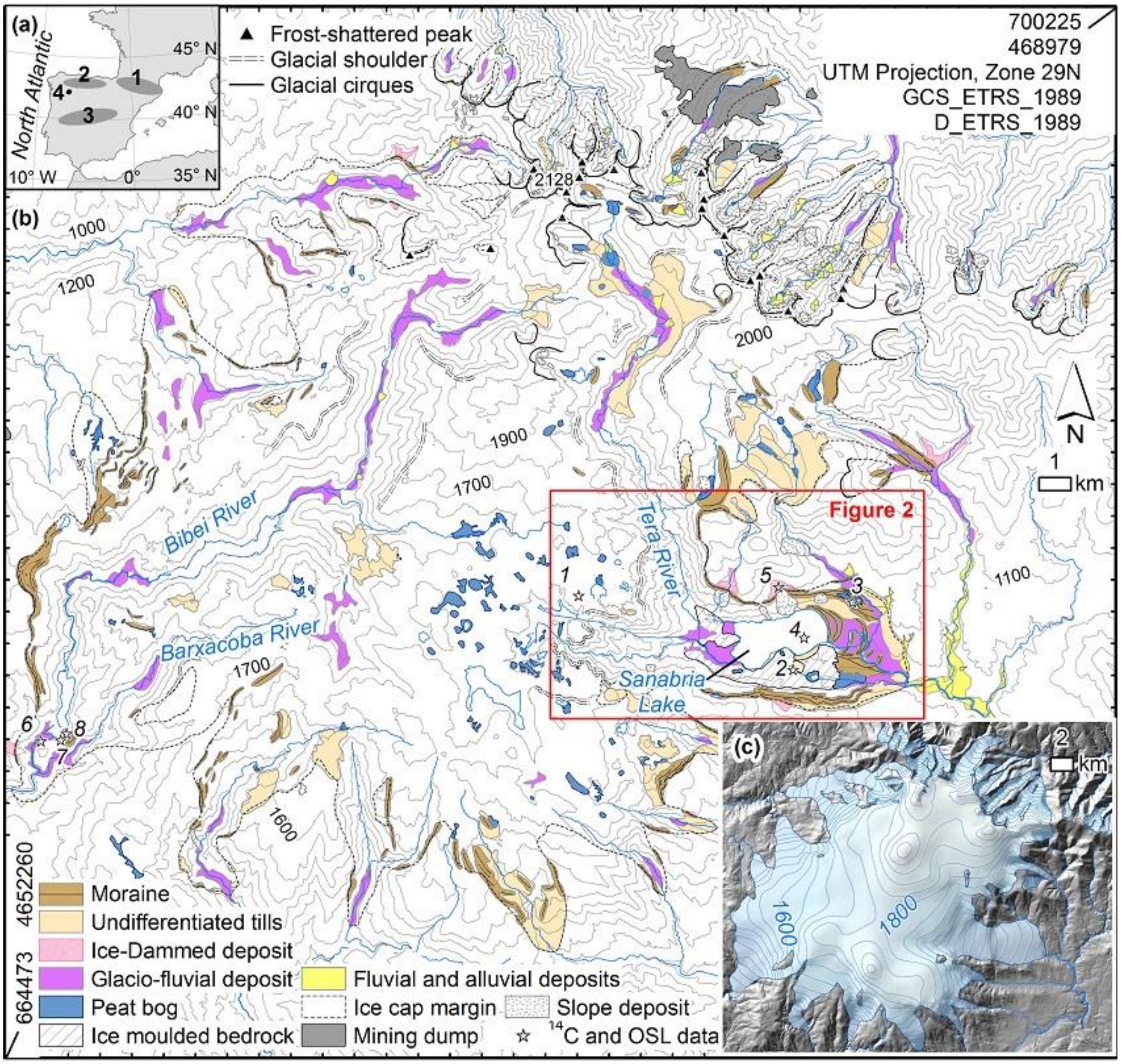

Figure 2. Geomorphological map of the Sanabria Lake area showing the location of the sampled boulders and the minimum exposure ages (^{10}Be) reported in this work, expressed in ka with the analytical (1σ) and external uncertainty for age comparisons with other datasets. Dates used to calculate the minimum ages for each moraine are represented in bold.

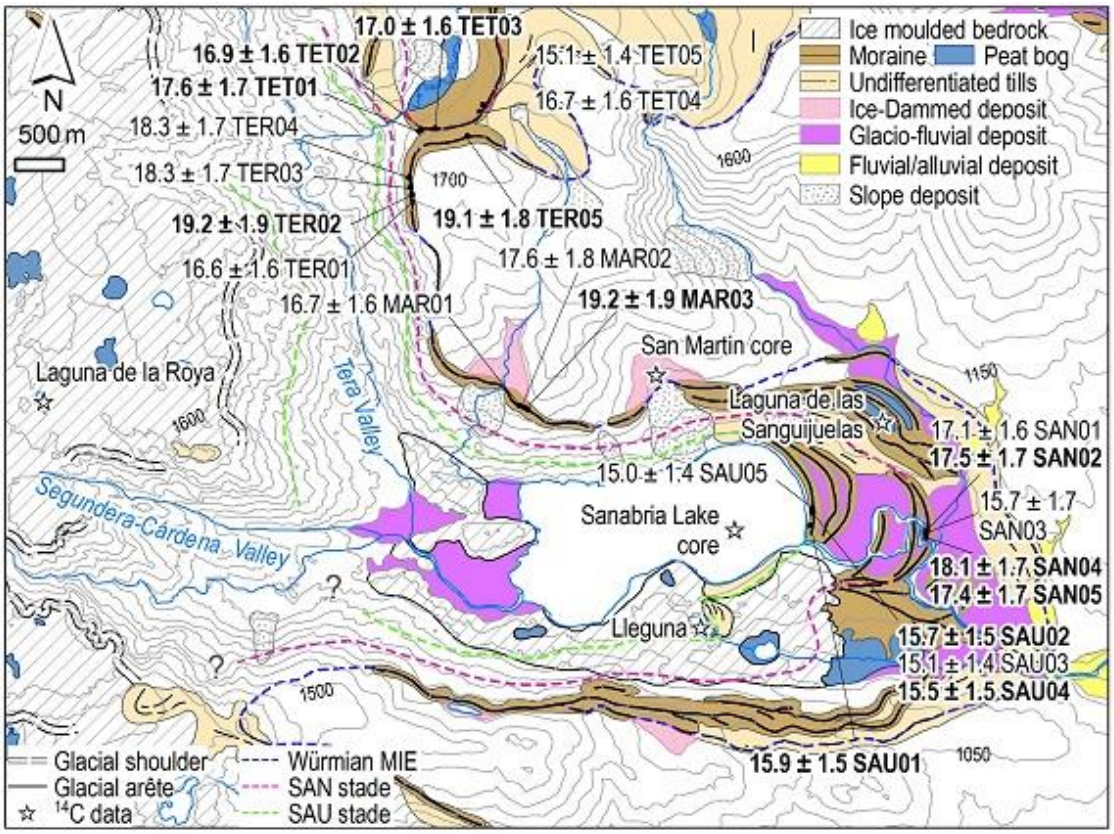

Figure 3. ^{10}Be exposure ages calculated with online CRONUS calculator (Balco et al., 2008; v. 2.2.1 updated in Balco, 2010). Samples are arranged from left to right according to distance from cirque headwall or ice dome (case of TET moraine). Black dots indicate which samples were used to derive moraine minimum exposure ages, while error bars indicate the analytical uncertainty (1σ) for each sample. Boulder ages are tightly grouped within each moraine.

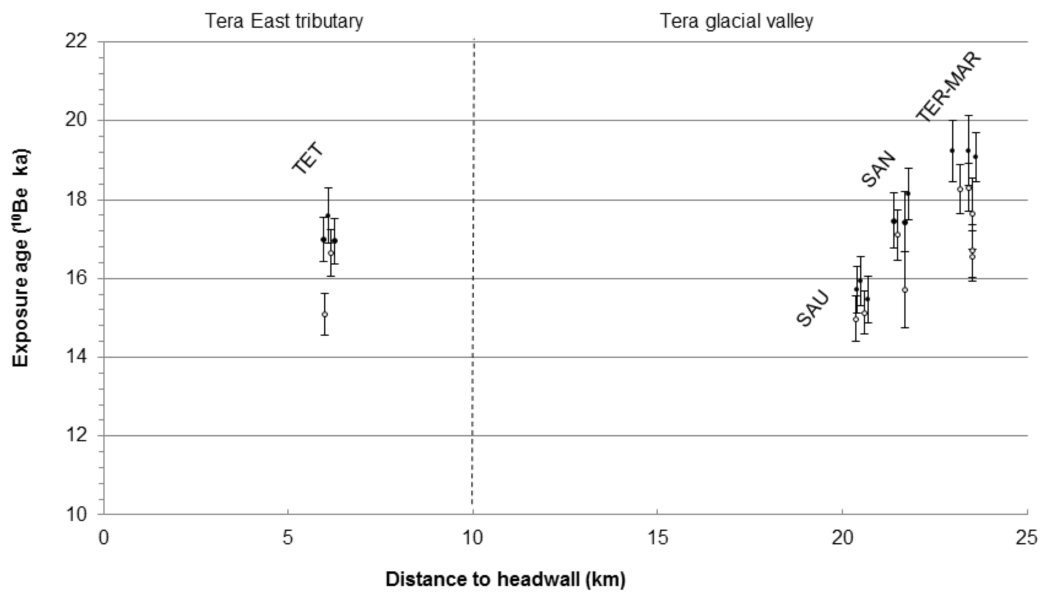

Figure 4. Examples of moraines sampled for the TCN analysis: (a) panorama of the TER moraine looking northwards, with TER01 in the foreground and the Tera valley in the background; (b) panorama of the MAR sample sites including one of the ice-dammed deposits formed behind the Sanabria Lake north lateral moraine; and (c) TET moraine panorama looking northeastward; including in the foreground the boulder where sample TET04 was collected. Boulder age uncertainties include only the analytical uncertainty.